

Spatiotemporal Control of Wave Instabilities in Cardiac Tissue

Wouter-Jan Rappel

Department of Physics, University of California, San Diego, La Jolla, California 92093

Flavio Fenton and Alain Karma

Department of Physics and Center for Interdisciplinary Research on Complex Systems, Northeastern University, Boston, Massachusetts 02115

(Received 30 November 1998)

Electrical waves circulating around an obstacle in cardiac tissue are subject to a generic oscillatory instability. In a one-dimensional ring geometry this instability can produce both quasiperiodic and spatiotemporally chaotic oscillations while in a two-dimensional sheet of cardiac tissue it can lead to spiral wave breakup. We present a control scheme to prevent this instability in these two geometries which is based on applying a feedback current at a discrete set of control points during the repolarizing phase of the action potential. The feasibility of this scheme is demonstrated via simulations of a two-variable model of excitable media with restitution and of the Beeler-Reuter model of ventricular action potential.

PACS numbers: 87.19.Hh, 05.45.Gg, 82.40.Ck

The propagation of a wave of action potential around a closed electrical circuit in the heart is one of the oldest mechanisms known to produce tachycardia, an abnormally rapid, albeit periodic, heart beat which is not controlled by the heart's natural pacemaker cells. Circulation can take place along a narrow ringlike pathway of active tissue surrounding a large obstacle, such as a vein or a large infarct (region of dead tissue resulting from a prior heart attack) [1]. It can also occur in the form of a spiral wave rotating in a large region of tissue, with the wave tip of the spiral meandering freely or being anchored on a small obstacle.

In recent years, it has become recognized that these waves can undergo various instabilities that can produce more complex arrhythmia and potentially induce ventricular fibrillation [2]. From a clinical standpoint, it is therefore desirable to develop means to control these instabilities using a finite number of electrodes implanted on the heart. Ideally, each electrode should deliver a small current comparable to the stimulus necessary to excite a cell, thereby avoiding the massive electrical shock of an implanted defibrillator.

In this Letter we present a scheme to control a generic oscillatory instability of cardiac excitation waves known to produce complex rhythms [3–5] and spiral wave breakups [6,7] at short circulation periods. Recent studies have focused on the *temporal* control of this instability in the atrioventricular nodal system [8–10]. In this context, it was shown that electrical alternans, the characteristic alternation of long and short action potential durations (APDs) associated with this instability, could be successfully suppressed using a global feedback scheme, and the feasibility of this scheme was demonstrated by Hall *et al.* [9] in an experiment. Here we focus on the *spatiotemporal* control of this instability in spatially extended geometries where the resulting wave dynamics is more complex. We investi-

gate the control of a pulse circulating in a one-dimensional (1D) ring of tissue, with alternans that are quasiperiodically modulated [3,4] or spatiotemporally chaotic [5], and of a spiral wave breakup induced by alternans in a 2D tissue. In both geometries, our scheme is able to prevent the instability to occur and to maintain stable periodic circulation with a vanishingly small control current.

Following standard cable theory, the propagation of electric waves in cardiac tissues can be described by

$$\frac{dV}{dt} = D \Delta V - I^{\text{ion}}/C_m, \quad (1)$$

where V is the transmembrane potential (mV), $D = 1 \text{ cm}^2/\text{sec}$ is the diffusion constant, and $C_m = 1 \text{ } \mu\text{F}/\text{cm}^2$ is the membrane capacitance. $I^{\text{ion}} (\mu\text{A}/\text{cm}^2)$ is the total membrane current density and describes the influx and efflux of ions through various ionic channels. Existing cardiac models differ in their description of I_{ion} . To demonstrate the robustness of our control scheme we study two different models in this Letter. One model, the Beeler-Reuter (BR) model [11], is a detailed cardiac model in which I_{ion} is the sum of four currents. The other model is a simplified two-variable (2V) model [6] with a fast variable that represents the membrane voltage and a slow variable that represents an effective membrane conductance [12]. The advantage of the latter model is that it incorporates the restitution property of cardiac cells (defined below) which is the cause of electrical alternans.

Our control method is based on applying a small control current, I^{con} , at a finite number, N_c , of equally spaced “controlled cells” in a tissue of N resistively coupled cells. Let us first consider the simplest case ($N_c = N = 1$) of an isolated periodically paced cell for which Eq. (1) reduces to

$$\frac{dV}{dt} = V_s \sum_{n=0}^{\infty} \delta(t - nT) - (I^{\text{ion}} + I^{\text{con}})/C_m. \quad (2)$$

The sum on the right-hand side of Eq. (2) represents the sequence of pacing stimuli at period T where $V_s \sim 10\text{--}20$ mV is the stimulus which must be large enough to excite a cell and I^{con} ($\mu\text{A}/\text{cm}^2$) is the control current. The motivation for first examining Eq. (2) is that it has the same period doubling bifurcation as a pulse circulating in a ring in the limit where the propagation speed of the wave front is constant in time. In this limit, space and time are effectively decoupled and each cell in the ring is reexcited at each passage of the wave front at a fixed period $T = L/c$, where L is the ring perimeter and c is the speed of the wave front. Without control ($I^{\text{con}} = 0$), the sequence, APD_n , of action potential durations generated by Eq. (2) can be described by the map [13,14]:

$$\text{APD}_{n+1} = F(T - \text{APD}_n), \quad (3)$$

where $\text{APD} = F(\text{DI})$ is the APD restitution curve that relates the action potential duration with the diastolic interval (DI), which is the interval between the time at which the action potential is initiated and the end of the previous action potential. This curve, to which the 2V model can be fitted, typically increases with DI, at short DI, and saturates to a constant value at large DI. Physiologically, this reflects the fact that the pulse duration is shorter when the cells are reexcited before recovering their resting state. The map loses its stability when the slope of the restitution curve is larger than one [13,14] as can be seen by linearizing Eq. (3) around the fixed point defined by $\text{APD}^* = F(\text{DI}^*)$, where $\text{DI}^* = T - \text{APD}^*$. Letting $\text{APD}_n = \text{APD}^* + \delta\text{APD}_n$, one obtains $\delta\text{APD}_{n+1} = -F'(\text{DI}^*)\delta\text{APD}_n$, which shows that the bifurcation occurs when $F'(\text{DI}^*) > 1$.

Our control scheme should stabilize not only the unstable fixed point of the map, as in previous works [8–10], but must also be generalizable to spatiotemporal control in a higher dimension. To this end we use a nonlinear version, with a “switch,” of a linear feedback scheme that has been successfully implemented in a variety of different systems [15]. It consists of comparing the present state of the system to the state at a time τ in the past. This is accomplished by choosing

$$I^{\text{con}} = \gamma(V(t) - V(t - \tau))\Theta(V(t) - V(t - \tau)), \quad (4)$$

where the delay time $\tau = T$ for the paced cell, and γ is a control parameter in mS/cm^2 . One important property of this scheme is that I^{con} is only nonzero transiently and vanishes in the controlled state where $V(t)$ is a periodic function with period T . The Heaviside step function, defined by $\Theta(x) = 1$ for $x \geq 0$ and $\Theta(x) = 0$ for $x < 0$ acts as a switch which turns on the feedback current only during the repolarizing phase of the action potential. This switch is not necessary to achieve control for the paced cell or the circulating pulse in the 1D ring. Our experience has shown, however, that it is necessary to control spiral wave breakup in 2D. Without the switch,

cells become excited by the control current for large enough γ , which promotes instability. The switch enables us to use larger values of γ without exciting cells.

To see why this scheme stabilizes the map defined by Eq. (3), let us assume that at the n th + 1 stimulus, $\text{APD}_{n+1} > \text{APD}_n$, which in turn implies that $V(t) > V(t - T)$. Therefore, according to Eq. (4), the control current will be switched on and lead to a faster repolarization of the membrane at a rate proportional to $V(t) - V(t - T) \sim \text{APD}_{n+1} - \text{APD}_n$. This will reduce APD_{n+1} by an amount proportional to $\text{APD}_{n+1} - \text{APD}_n$ and lead to the incremental change near the fixed point, $\delta\text{APD}_{n+1} \sim -\delta(\text{APD}_{n+1} - \text{APD}_n)$; or, equivalently, $\delta\text{APD}_{n+1} = \Gamma\delta\text{APD}_n$, where Γ is some effective control parameter that should be proportional to γ , for small γ . Adding this contribution to the change of APD resulting from restitution, we obtain that $\delta\text{APD}_{n+1} = [-F'(\text{DI}^*) + \Gamma]\delta\text{APD}_n$. At the next stimulus, the control current will be switched off because $\delta\text{APD}_{n+2} < \delta\text{APD}_{n+1}$, and therefore $\delta\text{APD}_{n+2} = -F'(\text{DI}^*)\delta\text{APD}_{n+1}$. Combining the above two expressions, we obtain the linearized map near the fixed point

$$\delta\text{APD}_{n+2} = F'(\text{DI}^*)[F'(\text{DI}^*) - \Gamma]\delta\text{APD}_n. \quad (5)$$

The condition for control to be achieved is that this map be stable, which yields $\Gamma > \Gamma_c$, where $\Gamma_c = [F'(\text{DI}^*)^2 - 1]/F'(\text{DI}^*)$. We have verified numerically for the 2V ionic model defined below that Γ is independent of T for a large range of values and that $\Gamma \sim \gamma$ for small γ . Thus, control requires $\gamma > \gamma_c$, where $\gamma_c \sim \Gamma_c \sim [F'(\text{DI}^*)^2 - 1]/F'(\text{DI}^*)$.

Let us now extend this scheme to spatiotemporal control of waves described by Eq. (1) with I^{ion} replaced by $I^{\text{ion}} + I^{\text{con}}$. In the 1D ring, the Laplacian is discretized in the form $\Delta V = (V_{i+1} + V_{i-1} - 2V_i)/dx^2$, where $x = idx$ measures the position along the ring of perimeter $L = Ndx$, and we impose the periodic boundary condition $V_{N+1} = V_1$. I^{con} , defined by Eq. (4), is applied at a subset of N_c equally spaced points along the ring, and $I^{\text{con}} = 0$ at the other points. In the 2D tissue, we use a square lattice of spacing dx with zero-flux boundary conditions at the edges and the discretized Laplacian $\Delta V = (V_{i+1j} + V_{i-1j} + V_{ij+1} + V_{ij-1} - 4V_{ij})/dx^2$. I^{con} is applied on a square superlattice of spacing $l = mdx$, resulting in $N_c = (N/m)^2$ control points with the first point placed at $(i = 1, j = 1)$. One difficulty, present in both geometries, is that the period T of unstable pulse circulation or spiral rotation is not known *a priori*. To overcome this problem, we choose τ equal to the average of the last two circulation periods at one point in the tissue (the position of this point is not essential). For this, we store the sequence of times, t_n , at which the membrane is depolarized (i.e., V exceeds some threshold value) at this point, and set $\tau = (t_n - t_{n-2})/2$ in Eq. (4) at all control points

during the interval, $t_n \leq t \leq t_{n+1}$. We find that using this scheme τ relaxes to T after a few periods and I^{con} vanishes in the final controlled state [16].

Results that illustrate control in the ring are shown in Fig. 1 for the BR and 2V models. Control in the 2D tissue is illustrated in Fig. 2 where we have purposely restricted our simulations to the 2V model in order to avoid the meander of the wave tip [7], which does not occur simultaneously with alternans in this model [6]. We expect that similar results would be obtained in a higher-order ionic model if the spiral wave tip is anchored on a small obstacle and does not meander. The equations were integrated using a simple Euler scheme with $dt = 0.05$ ms and $dx = 0.037$ cm in the 2V model, and $dt = 0.02$ ms and $dx = 0.0262$ cm in the BR model.

Figure 1 shows that the control scheme is robust and does not depend on a particular choice of model. We have also applied our scheme to a modified BR model developed by Qu *et al.* [5], which displays spatiotemporal chaos in a ring due to a nonmonotonic restitution curve. Using their model with the parameter $a = 0.75$ of Ref. [5], we verified that our control scheme can terminate the spatiotemporal chaotic oscillations of APD and force periodic circulation.

In Fig. 2, a stable spiral with a period of 200 ms was first created on a 200×200 ($7.4 \text{ cm} \times 7.4 \text{ cm}$) lattice for $S = 1.8$ (where S is defined in [12]). S was then increased abruptly to a value ($S = 2.4$) where, without control, the spiral is unstable and breaks up after a few rotations. In contrast, with control turned on one period

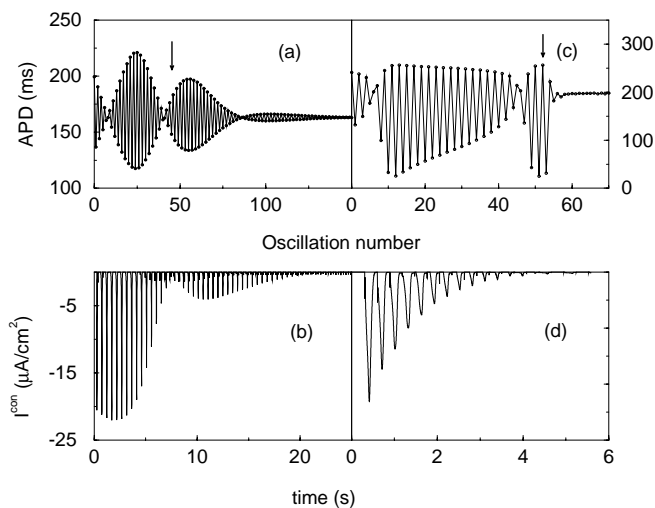


FIG. 1. Plots illustrating the control of a 1D pulse circulating in a ring for the 2V model with restitution [(a) and (b)] and the BR model [(c) and (d)]. For the 2V model, the ring perimeter $L = 4.26$ cm, $N_c/N = 0.026$, and $\gamma = 1.5$ mS/cm², and for the BR model, $L = 11.8$ cm, $N_c/N = 0.033$, and $\gamma = 0.6$ mS/cm². The APD is plotted as a function of the turn number in the ring in (a) and (c). Control is switched on at the turn number indicated by the arrows. The control current is plotted vs time in (b) and (d) with $t = 0$ corresponding to the start of control.

after the increase in S , the APD oscillations along the spiral arm are damped out and breakup is prevented. In addition, Figs. 1(b) and 1(d) demonstrate that a relatively small control current is necessary to achieve control. The maximum control current during the transient relaxation to the periodic state is about 5 times the maximum value of I^{ion} during membrane repolarization in both models ($\approx 5 \mu\text{A}/\text{cm}^2$) and about 1 order of magnitude smaller than the maximum value of I^{ion} during depolarization in the BR model ($\approx 135 \mu\text{A}/\text{cm}^2$).

The minimum control current, I_m , and the time, t_c , required to achieve control depend sensitively on the number of control points. We define I_m to be the peak oscillation amplitude of I^{con} during the transient after control is turned on, for the smallest γ necessary to achieve control (i.e., to reach steady-state rotation in some arbitrary long time). Figure 3 shows clearly that $I_m \sim 1/N_c$ in 1D. Remarkably, this scaling implies that the wave instability can be suppressed if $N_c I_m$ exceeds some threshold value, independently of whether the electrodes are equally spaced along the ring or regrouped in one segment, which we have checked numerically. As a result, control can be achieved in 1D with only one localized segment of controlled cells. The control time,

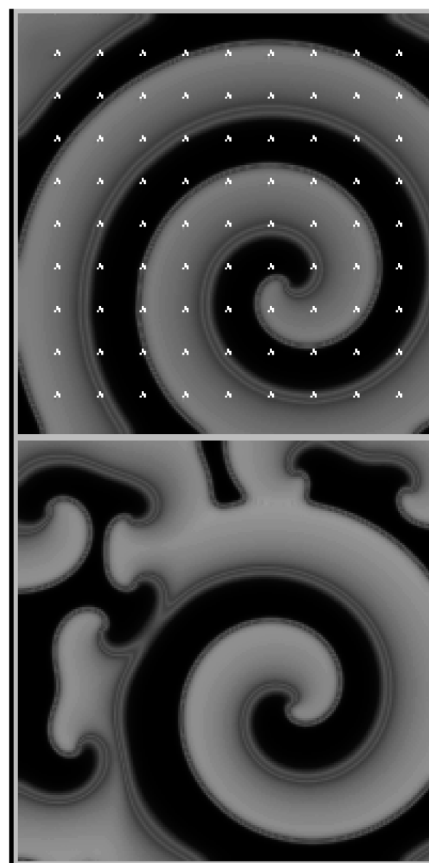


FIG. 2. Grey scale plot of voltage activity in a 2D tissue obtained by simulation of the 2V model without control after ten rotations (left), and with control in steady-state rotation (right) using $N_c/N = 0.0016$ and $\gamma = 32$ mS/cm².

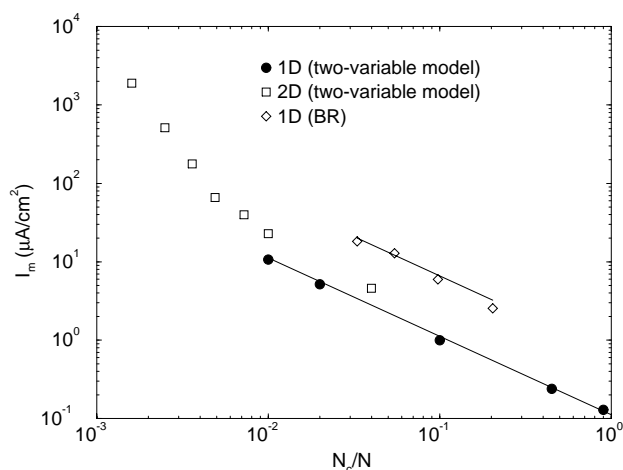


FIG. 3. Plot of I_m vs N_c/N for the different models in 1D and 2D. The straight lines are guides to the eye with a slope -1 .

however, depends on how the electrodes are placed along the ring. To investigate this, we have defined t_c to be the time necessary for the amplitude, $|\text{APD}_{n+1} - \text{APD}_n|$, of APD oscillations to decay to a small value δ after control is turned on. We find that for a fixed γ and N_c control points equally spaced along the ring, t_c is roughly N_c times smaller than with all points regrouped in one segment.

In 2D, Fig. 3 shows that I_m scales only as $1/N_c$ for large N_c . There are two distinct limiting factors present in 2D that are responsible for this difference. The first is that control must be achieved before breakup occurs, such that t_c must be less than the characteristic amplification time of the instability (a few rotations). Since we find that t_c decreases with increasing N_c in both 1D and 2D, this sets a lower bound on N_c in 2D. A similar bound is also present in 1D if we require that the amplitude of APD oscillations reaches some small desired value in a finite number of rotations. The second limiting factor in 2D is that the electrode spacing, l , must be comparable or smaller than the spiral wavelength, λ . This second factor causes I_m to increase rapidly at small N_c towards a range which is not practically interesting.

It would be interesting to test the present scheme experimentally in rings and sheets of tissue preparations. An array of electrodes that essentially performs the algorithm presented in this Letter (measure the potential, compare it to a previous potential and, if need be, deliver a small current) should be able to control wave instabilities. In rings, only one or a few electrodes should be required. In sheets, control of an anchored spiral wave should be possible with a coarse mesh of electrodes spaced about

1 cm apart. Since the control current is very small, the damage to the tissue should be minimal which would make the scheme interesting from a clinical point of view.

This research was supported by the American Heart Association.

-
- [1] D.P. Zipes and J. Jalife, *Cardiac Electrophysiology: From Cell to Bedside* (W.B. Saunders, Philadelphia, 1995); A. T. Winfree, *When Time Breaks Down* (Princeton University Press, Princeton, New Jersey, 1987).
- [2] For a review, see *Chaos* **8**, No. 1, 1 (1998).
- [3] L. H. Frame, R. L. Page, and B. F. Hoffman, *Circ. Res.* **58**, 495 (1986).
- [4] M. Courtemanche, L. Glass, and J. P. Keener, *Phys. Rev. Lett.* **70**, 2182 (1993); A. Karma, H. Levine, and X. Zou, *Physica (Amsterdam)* **73D**, 113 (1994).
- [5] Z. Qu *et al.*, *Phys. Rev. Lett.* **78**, 1387 (1997).
- [6] A. Karma, *Phys. Rev. Lett.* **71**, 1103 (1993); *Chaos* **4**, 461 (1994).
- [7] M. Courtemanche and A. T. Winfree, *Int. J. Bifurcation Chaos* **1**, 431 (1991); M. Courtemanche, *Chaos* **6**, 579 (1996).
- [8] D. J. Christini and J. J. Collins, *Phys. Rev. E* **53**, R49 (1996).
- [9] K. Hall *et al.*, *Phys. Rev. Lett.* **78**, 4518 (1997).
- [10] M. E. Brandt, H.-T. Shih, and G. Chen, *Phys. Rev. E* **56**, R1334 (1997).
- [11] For details on I^{ion} , see G. W. Beeler and H. Reuter, *J. Physiol. (London)* **268**, 177 (1977).
- [12] The 2V model is defined in the present units by
- $$I^{\text{ion}}/C_m = [V + 85 - (1 + 4\delta - n^M)f(V)]/\tau_V$$
- $$\partial_t n = \Theta(V + 60)(1 + S)/S - n/\tau_n,$$
- where $f(V) = \sum_{i=0}^3 c_i V^i$ with $c_0 = 72.83$ mV, $c_1 = -8.3 \times 10^{-1}$, $c_2 = -4.976 \times 10^{-2}$ mV $^{-1}$, $c_3 = -3.52 \times 10^{-4}$ mV $^{-2}$, $\delta = 0.22$, $\tau_V = 5$ ms, $\tau_n = 250$ ms, $S = 2.4$, $M = 15$ (1D), and $M = 4$ (2D).
- [13] J. B. Nolasco and R. W. Dahlen, *J. Appl. Phys.* **25**, 191 (1968).
- [14] M. R. Guevara, G. Ward, A. Shrier, and L. Glass, in *Computers in Cardiology* (IEEE Computer Society, Los Angeles, 1984), p. 167.
- [15] K. Pyragas, *Phys. Lett. A* **170**, 421 (1992); S. Bielawski, D. Derozier, and P. Glorieux, *Phys. Rev. E* **49**, R971 (1994); A. Kittel, K. Pyragas, and R. Richter, *Phys. Rev. E* **50**, 262 (1994); D. J. Gauthier *et al.*, *Phys. Rev. E* **50**, 2343 (1994); M. E. Bleich and J. E. S. Socolar, *Phys. Rev. E* **54**, R17 (1996).
- [16] We have also studied the case where a fixed input value of τ is used at all control points. In this case the scheme is still able to control alternans, but the final control current is zero only for the special choice $\tau = T$ and nonzero for all other choices.